THE EFFECT OF METAKAOLIN USED AS CEMENT REPLACEMENT ON THE PROPERTIES OF HARDENED CEMENT PASTE

Vaičekauskienė V.*, Nagrockienė D., Pundienė I.

Vilnius Gediminas Technical University, Sauletekio 11, Vilnius LT-10223, Lithuania

Abstract

The article analyses the effect of expanded glass production by-product rich in metakaolin on the properties of hardened cement paste. Portland cement CEM II/A-LL 42.5 N with the average particle size of 14.21 µm and metakaolin with the average particle size of 22.34 µm were used for the tests. Six cement paste compositions were formulated by replacing 0 %, 2 %, 4 %, 6 %, 8 %, 10 % of cement with metakaolin. Ultrasonic pulse velocity, compressive strength, flexural strength, water absorption and porosity of hardened cement paste specimens were measured at 28 days. The analysis of hardened cement paste microstructure (SEM) and physical and mechanical properties leads to the conclusion that the replacement of 8% of cement in the mix with metakaolin creates the densest microstructure that produces the highest values of compressive and flexural strengths and ultrasonic pulse velocity and the lowest values of closed porosity and water absorption rate. It was found that 8 % was the optimal ratio of cement replacement with metakaolin. Metakaolin can be added at 8 % by weight of cement in the production of modified high-performance concrete.

Keywords: *metakaolin, hardened cement paste, compressive strength, water absorption*

1. INTRODUCTION

Portland cement is currently one of the most commonly used concrete binders [1]. Portland cement has excellent strength characteristics and is resistant to freezing/thawing and water. However, high levels of carbon dioxide emission in Portland cement manufacturing are one of the greatest concerns nowadays [2]. This problem is addressed by investigations into materials that can reduce Portland cement content in the mixes without compromising or even improving the properties of the concrete. The use of various industrial by-products and waste would also address another relevant issue, namely waste recovery. Various studies on different types of waste and its use in the production of mortars and concretes are carried out.

Researchers studied metakaolin waste generated in foam glass pellet manufacturing process and found that it increases the strength and reduces the drying shrinkage of concrete. Other researchers also investigated the use of metakaolin waste in cement mixes. Elavarasan et al. carried out tests with metakaolin and ground granulated blast furnace slag and found that the replacement of 20% of cement with 10% of metakaolin and 10% of ground granulated blast furnace slag resulted in higher compressive and tensile strengths in comparison to not modified concrete [3-4].

Rajkumar R. et al. investigated the flexural strength of reinforced concrete elements by replacing part of cement with metakaolin and marble dust and found that metakaolin can be used in small quantities to replace cement in the mix [5]. Researchers investigated the effect of metakaolin on concrete and found that 15% was the optimal content of metakaolin used to replace cement in order to improve the properties of concrete [6].

Chandar et al. analysed the microstructure of metakaolin and determined the mechanical properties of concrete. The strength of concrete increased when 10% of cement was replaced with the materials analysed [7].

Mouli carried out tests on metakaolin and banana fibre and their effect on concrete. The results showed that the addition of 15% of metakaolin and 3% of banana fibre improved the properties of concrete [8].

Zhan et al. investigated the performance of high-performance concrete, in which part of cement was replaced with metakaolin in combination with other types of waste, such as fly ash, granulated blast furnace slag, glass and steel slag powder. The replacement of 10% cement by metakaolin and granulated blast furnace slag increased the compressive strength of concrete [9].

Researchers studied the hydration and mechanical properties of high-performance concrete incorporating limestone and metakaolin. The tests showed that metakaolin increased the mortar strength at 14 days and reduced the exothermic peaks and the heat of hydration throughout the entire hydration process. The mechanical properties and microstructure of concrete containing metakaolin were analysed in steam curing conditions [10-11].

Medjigbodo et al. analysed the effect of metakaolin and limestone on the properties of mortars and found that the optimal metakaolin content in the cement mix was 30%. The strength of mortars depends on the properties of metakaolin and its particle size distribution. The pozzolanic reaction accelerated with a lower w/c ratio and the early strength and durability parameters also improved [12].

Nepomuceno investigated cement mortars in which 50% of the cement was replaced by limestone, metakaolin, glass powder and ceramic waste. The results showed that a high content of minerals influences the properties of the mortar and can be used in mortar manufacturing [13].

Chand evaluated the properties of sustainable concrete made using a mixture of Portland cement, glass powder, metakaolin and silica fume. Experimental testing revealed the increase in the early strength, which decreased with time [14].

Researchers investigated the thermal conductivity of the cement mix modified with glass powder, metakaolin and limestone. The addition of metakaolin increased the thermal conductivity of cement by 54% and the compressive strength by 43% [15].

Researchers carried out a study on the performance of self-compacting concrete with waste glass aggregate and metakaolin. The addition of crushed glass deteriorated the mechanical properties of the concrete, while metakaolin, used as cement replacement, improved the mechanical properties of concrete [16-17].

Other researchers investigated the compressive strength of concrete using steel fibres in the mix and metakaolin as a partial substitute for the binder. They found that up to 10% of metakaolin used as cement replacement in the mix increased the strength of the concrete, while a higher metakaolin content decreased the compressive strength at 28 days compared to concrete without metakaolin [18].

The present paper analyses the effect of replacing cement by metakaolin waste and the amount of metakaolin waste used on the density, ultrasonic pulse velocity, flexural and compressive strengths, water absorption and porosity of hardened cement paste.

2. MATERIALS AND METHODS

2.1. Materials

Cement CEM II/A-LL 42.5 N complying with the requirements of LST EN 197-1 [19] and metakaolin by-product generated in foam glass pallet manufacturing were used for the tests. Chemical compositions of metakaolin and cement are presented in Table 1. Physical characteristics of metakaolin waste and cement are presented in Table 2.

	SiO_2	Al_2O_3	Na_2O	CaO	MgO	Fe_2O_3	K O_2	TiO_2	ZnO
Cement, %	14.8	3.47	0.097	61.6	3.37	2.61	1.12	0.249	0.022
Metakaolin waste,%	50.4	20.9	11.2	5.54	2.22	0.61	0.51	0.33	-
	SO_3	**P_2O_5**	**BaO**	**SrO**	**CeO**	**Cl**	**ZrO_2**	**CuO**	**MnO**
Cement, %	4.56	0.089	-	0.081	-	0.039	0.013	0.014	0.031
Metakaolin waste, %	0.12	0.08	0.03	0.024	0.019	0.017	0.011	-	-

Table 1. Chemical compositions, %

According to Table 1, SiO_2 (50.4%) is the prevailing element in the chemical composition of metakaolin waste and Al_2O_3 (20.9%) is the second most abundant compound.

Properties	Cement	Metakaolin waste
Specific surface area, cm^2/g	3819	7043
Particle density, kg/m^3	3130	2700
Bulk density, kg/m^3	1210	650

Table 2. Properties of cement and metakaolin waste, %

Fig. 1 illustrates the particle size distribution of cement and metakaolin waste. The size of particles was measured within the interval of 0.1–100 µm. The average size of metakaolin waste particles is 22.34 µm and the average size of cement particles is 14.21 µm.

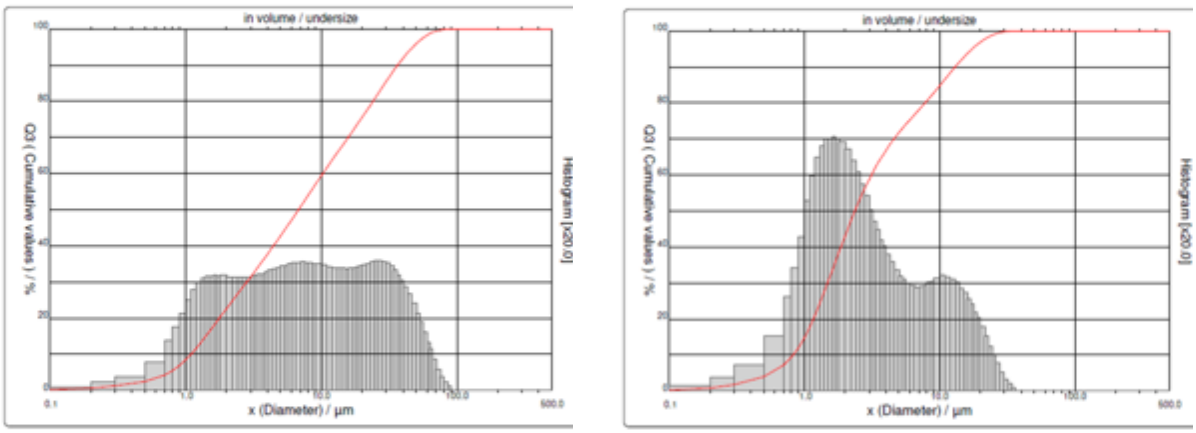

a) b)

Fig. 1. Particle size distribution of a) cement b) metakaolin waste

2.2. Methods

The chemical analysis of metakaolin waste was done by the X-ray fluorescence spectrometer Bruker X-ray S8 Tiger WD. The following spectroscopy parameters were used: Rh target X-ray tube, anode voltage *Ua* up to 60 kV, current *I* up to 130 mA. Pressed specimens were measured in helium atmosphere. SPECTRA Plus QUANT EXPRESS method was used for the measurements.

The structure of the materials was analysed by X-ray diffraction method (RSD or XRD). The chemical identification of compounds in the specimens was done by X-ray diffraction meter SmantLab (Rigaku) with a rotating Cu anode X-ray generator tube of 9 kW. The XRD patterns were plotted within the 2θ angle range from 5 to 75 degrees by using an optical system adjusted to Bragg-Brentano geometry, the sample rotating at 0.02 degree and the detector rotating at 1 degree per minute. The obtained data were analysed with PDXL (Rigaku) software using the Powder Diffraction File (PDF+) from ICDD (2021). The quantitative analysis of minerals was done by the RIR method [20].

Helios Nanolab 650 dual beam scanning microscope with focused ion beam (FIB) technology was used for SEM imaging [21]. The tests were done using the secondary electron image resolution with accelerating voltage of15 kV and electron beam current of 0.1 nA.

Compositions of hardened cement paste are presented in Table 3. Six compositions were formulated. A constant water/cement ratio (w/c) 0.3 was set for all compositions and in addition a chemical admixture was added at 0.4%. For each composition 2%, 4%, 6%, 8%, and 10% of cement was replaced with metakaolin.

The density of hardened cement paste specimens was measured according to LST EN 12390-7:2019 [22], the compressive strength was measured according to LST EN 12390-3:2019 [23], and the flexural strength was measured according to LST EN 12390-5:2019 [24].

Batches	**I**	**II**	**III**	**IV**	**V**	**VI**
Cement, %	100	98	96	94	92	90.
Water, %			100			
Metakaolin waste, %	0	2	4	6	8	10
Chemical admixture, %			0.4			
w/c			0.3			

Table 3. Mixing proportion of cement paste mixture

3. RESULTS AND DISCUSSION

The results of metakaolin waste X-ray diffraction analysis are presented in Figure 2. The XRD pattern (Figure 2) reveals that quartz has the highest peaks. Metakaolin waste also contains kaolinite, calcite and other minerals. Amorphous SiO_2 is the prevailing mineral in metakaolin waste. Metakaolin waste can be made of fine crystals because a wide peak is seen at 20-35 2-theta degrees.

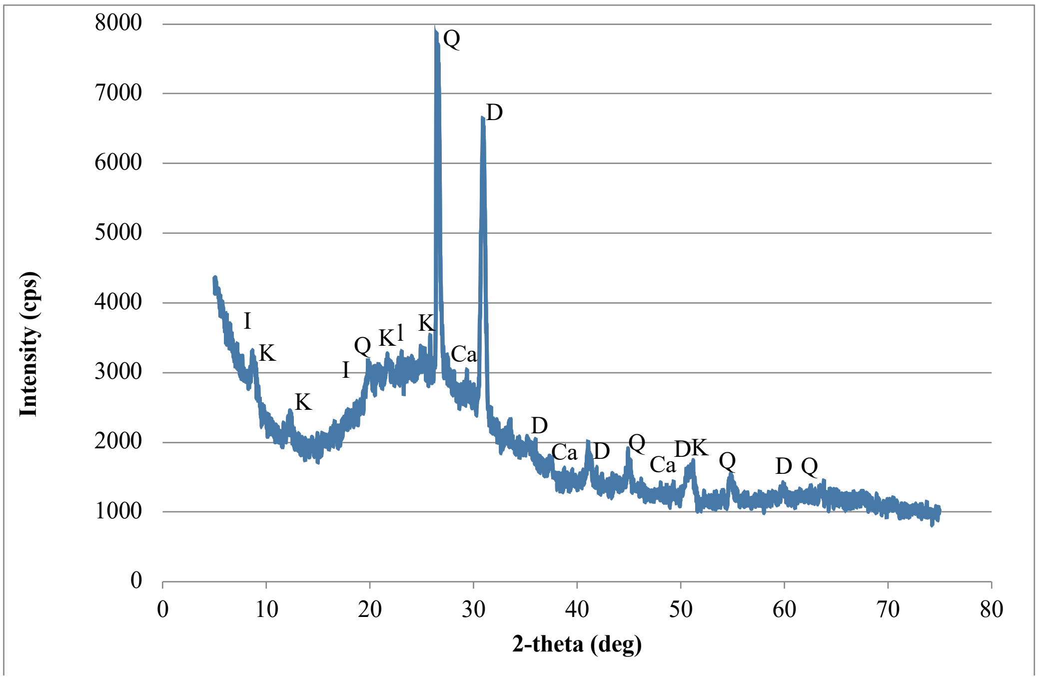

Fig. 2. XRD pattern of metakaolin; Q – quartz; D – dolomite; K – kaolinite; I – illite; Ca – calcite.

The microstructure of metakaolin waste is presented in SEM images in Figure 3. The SEM images reveal that metakaolin waste is made of round particles and irregular plate-shaped particles.

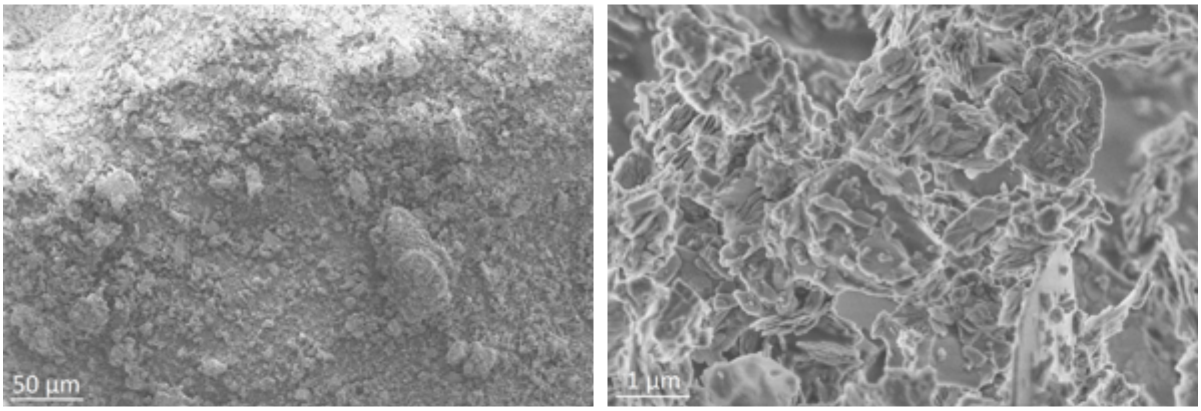

a) b)

Fig. 3. Microstructure of metakaolin waste: a) x500 magnification b) x25000 magnification

The results of hardened cement paste density tests are presented in Figure 4. The control specimen had the lowest density of 2072 kg/m^3 and the specimen containing 8% of metakaolin waste had the highest density of 2143 kg/m^3. A 3.43 % increase in density is observed. A slight drop in the density value to 2122 kg/m^3 was observed in specimens containing 10% of metakaolin waste. The hardened cement paste tests showed that only up to 8% of cement can be replaced with metakaolin waste.

Figure 4 illustrates the results of ultrasonic pulse velocity tests. The ultrasonic pulse velocity (UPV) in control specimens was 4149 m/s. The highest UPV value of 4210 m/s was observed in the specimens where 8 % of cement was replaced with metakaolin waste.

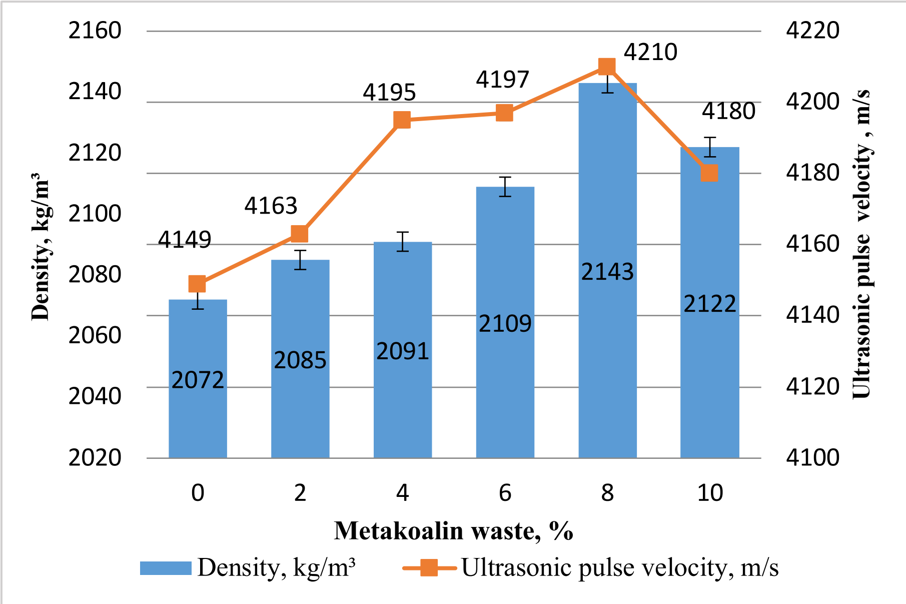

Fig. 4. Dependency of density and ultrasonic pulse velocity on the content of metakaolin waste

Compared with the control specimen, the UPV value in the specimen containing 8% of metakaolin waste increased 1.47 %. The replacement of 10 % of cement with metakaolin waste caused the UPV to decrease to 4180 m/s. This result indicates that up to 8% of cement can be replaced by metakaolin waste to increase the ultrasonic pulse velocity in hardened cement paste.

UPV values correlate with the density values. At higher density of hardened cement paste the UPV slightly increases and does not fall below the UPV value of control specimens.

Further analysis shows that the highest flexural strength of 12.2 MPa was achieved in hardened cement paste where 8 % of cement was replaced by metakaolin waste, whereas the flexural strength of control specimens was 6.5 MPa (Fig. 5), showing the increase of 53.28 %. The results presented in Figure 5 show that the flexural strength of hardened cement paste improves with the increase of metakaolin waste content up to 8 %. At 10 % replacement of cement with metakaolin waste, the flexural strength drops to 10.6 MPa.

According to the hardened cement paste strength results presented in Figure 5, the control specimen had the compressive strength of 62.3 MPa and the highest compressive strength of 81.3 MPa was observed in the specimens containing 8 % of metakaolin waste. The increase in compressive strength is 30.5 %. A further increase in metakaolin waste content to 10 % causes the compressive strength to decrease to 73.9 MPa.

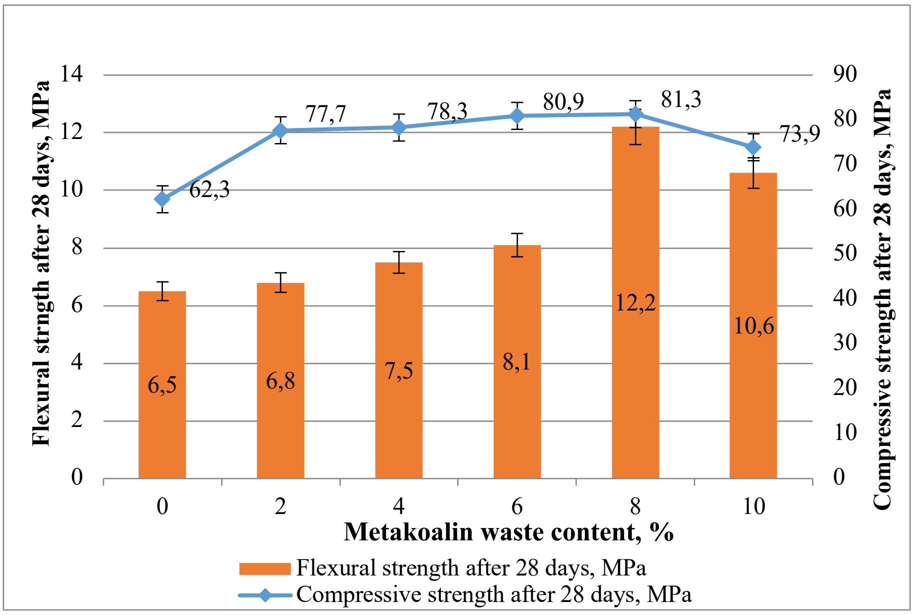

Fig. 5. The dependency of compressive and flexural strength of hardened cement paste on metakaolin content

The results of hardened cement paste absorption tests are presented in Figure 6. The control specimen had water absorption of 16.5 % and the lowest absorption of 14.5 % was observed in hardened cement paste where 8 % of cement was replaced by metakaolin waste. The porosity decreased 14.8 % compared to the control specimen. When 10 % of the cement was replaced by metakaolin waste, the water absorption increased to 15 %.

The porosity tests of hardened cement paste were carried out (Figure 6). The open porosity of hardened cement paste specimens decreased 14.78 % from 30.3 % in the control specimen to 26.4 % in the specimen where 8 % of the cement was replaced by metakaolin waste. 10 % of metakaolin waste in the mix caused the open porosity of hardened cement paste to increase.

The results of closed porosity test presented in Figure 6 show the change in the closed porosity of hardened cement paste. The closed porosity of the control specimen was 1.4 %. The closed porosity of the specimen where 10 % of cement was replaced by metakaolin waste increased to 6.5 %. The results show that the closed porosity increases with the increase of metakaolin waste content up to 10 %.

The total porosity of the control specimen of hardened cement paste was 31.7 %. The highest total porosity of 33.5 % was observed in the specimen containing 8 % of metakaolin waste. The total porosity increased 5.68 % compared to the control specimens (Figure 6). With the increase of metakaolin waste content to 10 %, the total porosity decreased to 33.3 %.

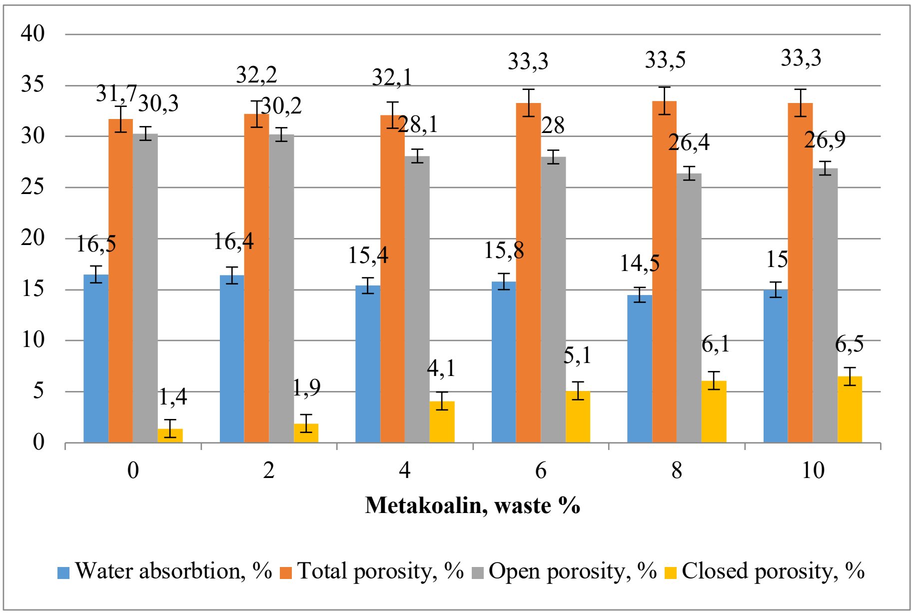

Fig. 6. Porosity characteristics of hardened cement paste depending on the amount of metakaolin waste.

The X-ray diffraction analysis of hardened cement paste specimens was done at 28 days. The analysis results are presented in Figures 7 and 8. The XRD pattern of the control specimen is given in Figure 7 and the XRD pattern of the specimen where 8 % of cement is replaced by metakaolin waste is given in Figure 8. The phases were determined in comparison with XRD patterns of the standard diffraction models provided by the International Centre of Diffraction Data (ICDD): portlandite (ICDD Card No 1–1079), ettringite (ICDD Card No 31–251), calcite (ICDD Card No 4–636), quartz (ICDD Card No 46-1045), calcium silicate hydrate (ICDD Card No 33-306).

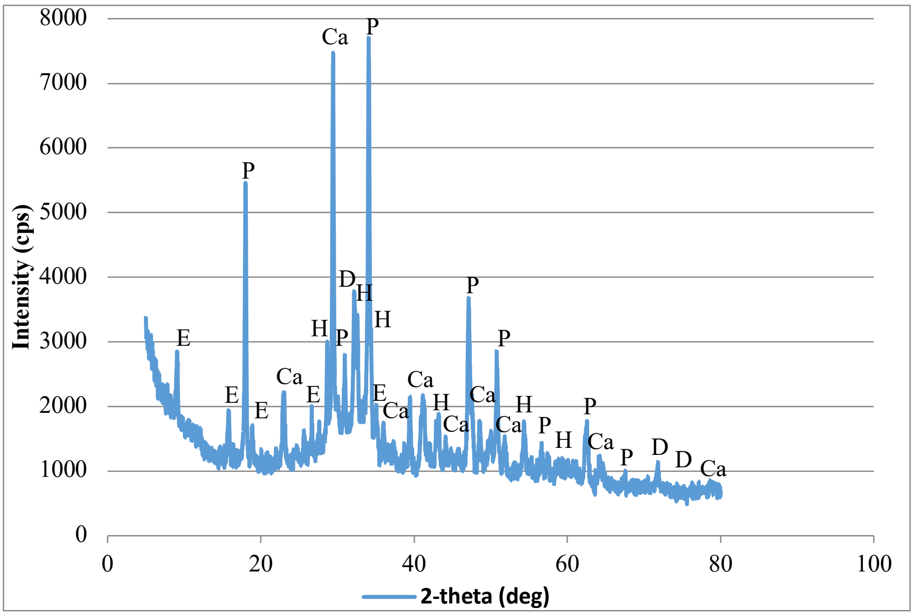

Fig. 7. XRD pattern of hardened Portland cement paste: D – dolomite; Ca – calcite; H – calcium silicate hydrate; P – Portlandite; E – ettringite; Q – quartz.

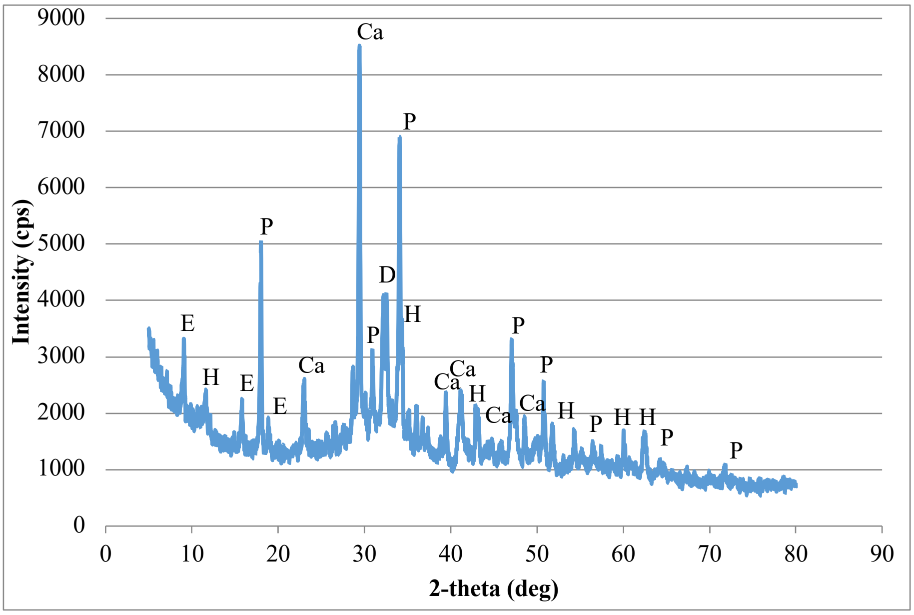

Fig. 8. XRD pattern of hardened cement paste containing 8% of metakaolin waste: D – dolomite; Ca – calcite; H – calcium silicate hydrate; P – Portlandite; E – ettringite; Q – quartz.

The most intensive CSH peak is observed in the specimen where 8 % of cement was replaced by metakaolin waste. More CSH is produced with the increase of the amorphous phase. The levels of calcite also depend on the amount of cement in the mix composition and tend to decrease because less $Ca(OH)_2$ is formed in the specimens and it can react with CO_2 present in the ambient air. The intensity of portlandite is lower in the specimens where 8 % of cement is replaced by metakaolin waste, whereas in control specimens the intensity of portlandite is higher. It can be concluded that the replacement of 8 % of cement by metakaolin waste causes the amorphous phase to increase and, subsequently, more CSH is formed despite the lower cement content of the specimen.

SEM images of the control hardened cement paste specimen and the specimen containing 8 % of metakaolin waste are given in Figure 9. The images reveal larger pores in the control specimen and denser structure of the specimen where 8 % of cement is replaced by metakaolin waste.

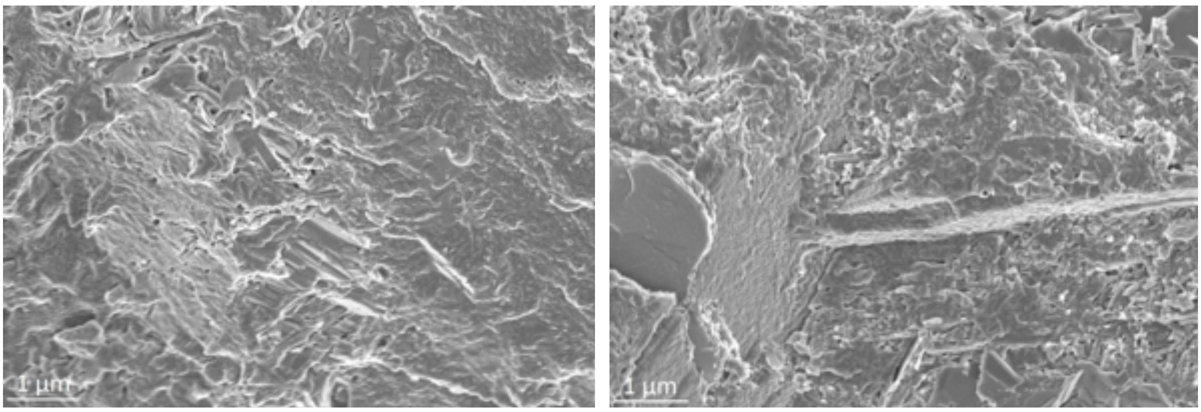

a) b)

Fig. 9. Microstructure of hardened cement paste: a) control specimen x2500 magnification b) specimen with 8% of metakaolin waste x25000 magnification

4. CONCLUSIONS

Metakaolin waste has a positive effect on the modified hardened cement paste: better microstructure, increased amorphous phase and subsequently more CSH formed, thus improved physical and mechanical properties.

The analysis of physical and mechanical properties of hardened cement paste revealed that at 28 days the density, ultrasonic pulse velocity, flexural and compressive strength, and closed porosity values of the specimen where 8 % of cement was replaced by metakaolin waste increased, whereas water absorption decreased. The improvement of these properties in the specimens modified with metakaolin waste improved as a result of more intensive hydration and higher levels of hydration products formed, which was confirmed by XRD analysis results.

Water absorption was the lowest in hardened cement paste specimens where 8 % of cement was replaced by metakaolin waste compared to the control specimens without metakaolin waste. The specimen modified with 8 % of metakaolin waste had 13.79 % lower water absorption rate compared to the control specimen. Lower water absorption can be explained by the denser microstructure of the modified hardened cement paste.

The replacement of cement by 8 % of metakaolin waste produces a stronger and denser hardened cement paste that can be used in producing modified concrete utilising metakaolin waste.

REFERENCES

1. Scrivener, K.L., Snellings, R. 2022, The Rise of Portland Cements, *Elements*, vol. 18, no. 5, pp. 308-313.
2. Fayomi, G.U., Mini, S.E., Fayomi O.S.I., Ayoola, A.A., 2019, Perspectives on environmental CO_2 emission and energy factor in Cement Industry, *IOP Conference Series: Earth and Environmental Science*, vol. 331.
3. Jamal, M.K., Oussama, B., Adel, A.E, 2018, Waste and Supplementary Cementitious Materials in Concrete, Metakaolin, ch. 15. p. 493-511.
4. Elavarasan, S., Priya, A.K., Ajai, N., Akash, S., Annie, T.J., Bhuvana, G., 2021, Experimental study on partial replacement of cement by metakaolin and GGBS, *Materials Today: Proceedings,* vol. 37, pp. 3524-3530.
5. Rajkumar, R., Umamaheswari, N., Kumar, A., Kumar, M., Vineeth Gupta, L.R., Pandey, R., 2021, Flexural behaviour of reinforced concrete beams with partial replacements of metakaolin and marble powder, *Materials Today: Proceedings*, vol. 34, pp. 550-555.
6. Bright Singh, S., Murugan, M., 2022, Effect of metakaolin on the properties of pervious concrete, *Construction and Building Materials,* vol. 346.
7. Chandar, S.P., Santhosh, R., 2022, Mechanical properties and microstructural analysis of metakaolin and alccofine in M40 grade concrete, *Materials Today: Proceedings*, vol. 68, pp. 50-55.
8. Mouli, K.C., Pannirselvam, N., Anitha. V., Kumar, D.V., Rao, S.V., 2019, Strength studies on banana fibre concrete with metakaolin, *International Journal of Civil Engineering and Technology*, vol. 10, no. 2, pp. 684-689.
9. Zhan, P., 2021, Multi-scale study on synergistic effect of cement replacement by metakaolin and typical supplementary cementitious materials on properties of ultra-high-performance concrete, *Construction and Building Materials*, vol. 307.
10. Mo, Z., 2020, Hydration and mechanical properties of UHPC matrix containing limestone and different levels of metakaolin, *Construction and Building Materials*, vol. 256.
11. Mo, Z., 2021, Mechanical performances and microstructures of metakaolin contained UHPC matrix under steam curing conditions, *Construction and Building Materials*, vol. 268.

12. Medjigbodo, G., 2018, Hydration, shrinkage, and durability of ternary binders containing Portland cement, limestone filler and metakaolin, *Construction and Building Materials*, vol. 183, pp. 114-126.
13. Nepomuceno, M.C.S., 2021, Cement-based grouts for masonry consolidation with high content of limestone filler, metakaolin, glass powder and ceramic waste, *Construction and Building Materials*, vol. 306.
14. Chand, G., 2021, Assessment of the properties of sustainable concrete produced from quaternary blend of portland cement, glass powder, metakaolin and silica fume, *Cleaner Engineering and Technology*, vol. 4.
15. Du, Y., Yang, W., 2021, Thermal conductivity of cement paste containing waste glass powder, metakaolin and limestone filler as supplementary cementitious material, *Journal of Cleaner Production,* vol. 287.
16. Meraz, M.M., 2023, Performance evaluation of high-performance self-compacting concrete with waste glass aggregate and metakaolin, *Journal of Building Engineering*, vol. 67.
17. Singh, H., Siddique, R., 2022, Utilization of crushed recycled glass and metakaolin for development of self-compacting concrete, *Construction and Building Materials*, vol. 348.
18. Basavaraj, D.S., Ravikumar, M.S., 2022, Strength characteristics of concrete by utilization of metakaolin and steel fibers as partial substitute to binding material, *Materials Today: Proceedings*, vol. 60, p. 715-723.
19. LST EN 197-1:2011. Cementas. 1 dalis. Įprastinių cementų sudėtis, techniniai reikalavimai ir atitikties kriterijai // Lietuvos standartizacijos departamentas.
20. Madsen, I.C., Scarlett, N.V.Y., Kleebergb, R., Knorrc, K., 2019, International Tables for Crystallography, Reference intensity ratio methods, ch. 3.9, p. 347.
21. Pereira-da-Silva, M.A., Ferri, F.A., 2017, Nanocharacterization Techniques, Scanning Electron Microscopy, ch. 1, p. 1-35.
22. LST EN 12390-7:2019, Testing hardened concrete - Part 7: Density of hardened concrete.
23. LST EN 12390-3:2019, Testing hardened concrete - Part 3: Compressive strength of test specimens.
24. LST EN 12390-5:2019, Testing hardened concrete - Part 5: Flexural strength of test specimens.